Modeling of Size Quantization in Strained Si-nMOSFETs with the Improved Modified Local Density Approximation.

C. D. Nguyen, C. Jungemann, and B. Meinerzhagen

NST, Technical University Braunschweig, Postfach 3329 Braunschweig, Germany, c-d.nguyen@tu-bs.de

ABSTRACT

An Improved Modified Local Density Approximation - (IMLDA) model for the electron inversion layer in strained Si-nMOSFETs is presented which correctly describes the impact of size quantization on the threshold voltage and capacitance without increasing the computation time. The IMLDA model yields results consistent with the self-consistent solution of the Schrödinger and Poisson equations (SE/PE) for a wide range of strain, temperature and doping concentrations. A big advantage of the IMLDA model is its low computation time and its numerical robustness, because it depends only on local quantities and not on solution variables of the numerical model. Additionally, this model is well suited for software implementation in existing TCAD device simulators.

Keywords: Strained Si, MOS devices, Quantization effects, Inversion layer

1 INTRODUCTION

The change in the band structure due to strain has a strong impact on size quantization in the inversion layer which has to be taken into account in device modeling in order to obtain the correct inversion charge density, which impacts directly the threshold voltage and gate capacitance of MOSFETs. This can be done with high accuracy on the level of the Schrödinger equation (SE). However, solving the SE in a TCAD device simulator is very CPU intensive and leads to numerical problems[1], [2]. Therefore, simple and more efficient approximate quantum correction models have been developed (e.g. the IMLDA model [1] and the density gradient model DGM [2]), but only for the case of unstrained Si. The first DGM for electrons in strained Si was introduced in [3]. The DGM is able to predict both the correct threshold voltage and the density distribution in the device, but it is numerically more challenging [2], [4] and CPU intensive than the classical model. In contrast to the DGM, the model presented in this work for electrons in strained Si is based on the IMLDA model [1], which does not depend on the electrostatic potential or any other solution variable of the device model. Therefore, the convergence properties and the CPU time efficiency of the classical model without quantum correction are maintained by our new model. In most practical cases the IMLDA model is about 7 times faster than the DGM.

2 IMLDA MODEL

The IMLDA model for electrons in strained Si has been developed similar to the model for unstrained Si [1]. The calculation of the electron density with the IMLDA model is based on

$$n(z) = \sum_{\nu=1}^{6} N_c^{\nu} \cdot \exp\left(\frac{E_F - qV_c^{\nu} - q\Psi_{\text{qm}}}{k_B T}\right) \qquad (1)$$

with

$$\Psi_{\text{qm}} = -\frac{k_B T}{q} \ln\left(1 - \frac{1}{3}\exp(-(\lambda_l z)^2) - \frac{2}{3}\exp(-(\lambda_t z)^2)\right) \qquad (2)$$

$$V_c^{\nu} = \Psi + \frac{\Delta E_c^{\nu}}{q}, \qquad (3)$$

where N_c^{ν} is the effective density of states in ν-th valley, T the lattice temperature, $\lambda_{l/t} = \sqrt{\frac{2m_{l/t}k_B T}{\hbar^2}}$ the inverse wave length, z the distance from the interface and Ψ_{qm} the corresponding quantum potential. The potential V_c^{ν} is the sum of the electrostatic potential Ψ and the conduction band edge ΔE_c^{ν} in the respective valley. The conduction band edge step at the strained Si/Si$_{1-y}$Ge$_y$ interface is given by [6].

2.1 Inversion layer case

For the development of the IMLDA model reference data (the sheet charge of the inversion layer) were generated using the self-consistent solution of the Schrödinger and Poisson equations (SE/PE) for a large range of lattice temperatures T, doping levels N_{dop}, strained Si thicknesses t_{SSi} and Ge contents y (see Tab. 1). The reference data are needed for the parameter fitting of the IMLDA model. In indirect semiconductors like Si and Ge, the size quantization of the quasi-2D electron gas can be well described by a one band SE employing effective masses [3].

Similar to Ref. [1] the IMLDA model for strained Si is based on the modification of the inverse wave length parameters $\lambda_{l/t}$ in Eqn (2), which is determined by matching the reference data. In order to improve the model accuracy, the dependence of $\lambda_{l/t}$ on the distance from the surface was separated from its dependence on other local quantities with a different ansatz in comparison to Ref. [1]:

$$\lambda_{\text{mod.}} = \lambda_{l/t} \frac{(z/z_n)^{1200/T}}{(z/z_n)^{1200/T} + 1}\zeta \qquad (4)$$

T [K]	y	t_{SSi} [nm]	N_{dop} [cm^{-3}]
200	0.1	1	$1 \cdot 10^{17}$
250	0.2	2	$3 \cdot 10^{17}$
300	0.3	3	$5 \cdot 10^{17}$
350	0.4	4	$7 \cdot 10^{17}$
400	0.5	5	$1 \cdot 10^{18}$
450	0.6	8	$3 \cdot 10^{18}$
500	0.7	10	$5 \cdot 10^{18}$

Table 1: Discrete values of T, y, t_{SSi}, N_{dop} for which the reference data were calculated.

with $z_n = 1$ [nm], $m_{l/t} = 0.92/0.19 m_0$. Here, m_0 is the free electron mass and ζ a local fit-factor. For given doping, temperature, Ge content and strained Si thickness, ζ was extracted by a least square fit of the IMLDA results to the reference data. It is found that for $t_{SSi} \geq 4$nm the dependence of the fitting parameters on t_{SSi} can be neglected. Moreover the fitting parameters are independent of y for $y \geq 0.3$.

For TCAD use, the parameter ζ must be approximated by functions of the local quantities on the basis of the above extracted discrete values ζ (see table 2 in the Appendix). In contrast to the case of unstrained Si [1] the use of an analytic function for this approximation has been abandoned and has been replaced by a sequence of 1D-spline interpolations [5]. The advantage of this interpolation algorithm is high accuracy and high flexibility e.g. for a new shape of equation (4).

2.2 Polysilicon case

Similar to the IMLDA model for the strained Si inversion layer, an IMLDA model for the poly gate was developed in order to consider the quantization effects in the gate as well. For this case the reference data were generated with the one band SE for electrons and holes between 200 K and 500 K and n^+ polysilicon doping levels between $5 \cdot 10^{18}$ cm^{-3} and $5 \cdot 10^{20}$ cm^{-3}. Moreover the total sheet charge density at the poly/oxide interface which is direct proportional to the oxide field was chosen as the quantity of interest for the fitting procedure. Since the modeling of polysilicon is of minor importance for the overall accuracy, the application of the one band SE for polysilicon turned out to be sufficient even for the modeling of holes. The discrete fitting parameters are shown in table 3.

3 RESULTS

Figure 1 illustrates the inversion charge density N_{inv} as a function of the gate voltage for three different back biases. The Ge content in the relaxed buffer is 25%, the strained Si thickness 10nm, the gate oxide thickness 1.5nm, and a metal gate is used. Very good agreement is found between the IMLDA and the quantum mechanical reference model (SE/PE). To demonstrate that the IMLDA model yields good results for many different operation conditions and different devices, the comparison of the IMLDA with the SE/PE is repeated for other temperatures and other relevant doping levels and Ge contents (see Fig. 2, 3 and 4). The results confirm the universality and reliability of the IMLDA model.

Fig. 5 and 6 show the inversion charge density calculated by the IMLDA and the SE/PE for different doping concentrations, and a polysilicon gate where the quantization effect in the polysilicon is considered. Again, good agreement is found between the IMLDA model and SE/PE. These results confirm the reliability of the IMLDA model for modeling of size quantization both in the inversion layer and in the poly gate.

Please note that for this IMLDA model verification germanium contents y as well as doping levels have be chosen which were not considered during the IMLDA model development.

4 CONCLUSIONS

We have presented the first accurate local electron charge density approximation for quantization effects in the inversion layer and poly gate of strained Si-nMOSFETs. The model shows excellent agreement with the reference model for a wide range of Ge content, temperature and channel doping.

5 ACKNOWLEDGMENTS

We'd like to thank the Semiconductor Research Corporation (SRC) for financial support under task number ID 1144.001.

REFERENCES

[1] C. Jungemann, C. D. Nguyen, B. Neinhüs, S. Decker and B. Meinerzhagen, "Improved Modified Local Density Approximation for Modeling of Size Quantization in NMOSFETs", *MSM'2001*, (USA), pp. 458–461, 2001.

[2] A. Wettstein, A. Schenk and W. Fichtner, "Quantum Device-Simulation with the Density-Gradient Model on Unstructured Grids", *IEEE Trans. Elec. Dev.*, **48**(2), 279–284, 2001.

[3] C. D. Nguyen, A. T. Pham, C. Jungemann and B. Meinerzhagen, "Study of Charge Carrier Quantization in Strained Si-nMOSFETs", *Materials Science in Semiconductor Processing*, Vol. 8, pp. 363–366, 2005.

[4] M. G. Ancona and B. A. Biegel, "Nonlinear Discretization Scheme for the Density-Gradient Equations", *SISPAD'2000*, (USA), pp. 196–199, 2000.

[5] H. Akima, "A Method for Univariate Interpolation that Has the Accuracy of a Third-Degree Polynomial", *ACM Transactions on Mathematical Software*, vol. 17, pp. 183-192, 1991

[6] F. Schäffler, "High–mobility Si and Ge structures", *Semicond. Sci. Technol.*, vol. 12, pp. 115-1549, 1997.

APPENDIX

T[K] \ N [cm^{-3}]	$1 \cdot 10^{17}$	$3 \cdot 10^{17}$	$5 \cdot 10^{17}$	$7 \cdot 10^{17}$	$1 \cdot 10^{18}$	$3 \cdot 10^{18}$	$5 \cdot 10^{18}$
200	0.88	0.88	0.89	0.89	0.90	0.90	0.88
250	0.99	1.01	1.04	1.06	1.09	1.15	1.15
300	1.08	1.11	1.14	1.17	1.20	1.31	1.33
350	1.16	1.19	1.23	1.26	1.30	1.42	1.45
400	1.23	1.27	1.30	1.33	1.36	1.49	1.53
450	1.31	1.33	1.36	1.39	1.42	1.55	1.59
500	1.38	1.40	1.42	1.44	1.47	1.59	1.64
$y = 0.1$							
200	1.88	1.79	1.74	1.71	1.68	1.58	1.51
250	2.12	2.12	2.11	2.11	2.09	2.02	1.96
300	2.23	2.30	2.32	2.34	2.34	2.30	2.25
350	2.28	2.38	2.42	2.45	2.47	2.47	2.41
400	2.28	2.39	2.45	2.48	2.52	2.56	2.51
450	2.28	2.38	2.43	2.48	2.52	2.59	2.56
500	2.27	2.35	2.41	2.45	2.49	2.58	2.57
$y = 0.2$							
200	1.97	1.87	1.81	1.78	1.74	1.62	1.56
250	2.39	2.35	2.32	2.30	2.27	2.14	2.08
300	2.73	2.74	2.72	2.70	2.69	2.55	2.43
350	2.98	3.02	3.02	3.00	3.00	2.85	2.72
400	3.14	3.20	3.20	3.20	3.19	3.06	2.93
450	3.22	3.29	3.30	3.31	3.30	3.20	3.07
500	3.23	3.31	3.34	3.35	3.35	3.27	3.16
$y = 0.3$							
200	1.97	1.87	1.81	1.78	1.75	1.63	1.57
250	2.40	2.36	2.33	2.31	2.28	2.15	2.09
300	2.78	2.78	2.76	2.74	2.72	2.58	2.45
350	3.11	3.13	3.12	3.10	3.07	2.91	2.77
400	3.36	3.41	3.39	3.37	3.35	3.17	3.02
450	3.54	3.60	3.59	3.57	3.55	3.37	3.22
500	3.65	3.73	3.72	3.71	3.69	3.51	3.36

Table 2: Discrete values of the fitting parameters for the inversion layer.

T[K] \ N [cm^{-3}]	$5 \cdot 10^{18}$	$1 \cdot 10^{19}$	$2 \cdot 10^{19}$	$5 \cdot 10^{19}$	$1 \cdot 10^{20}$	$2 \cdot 10^{20}$	$5 \cdot 10^{20}$
200	1.14	1.19	1.28	1.49	1.69	1.80	1.28
250	1.20	1.26	1.37	1.65	2.00	2.41	2.46
300	1.24	1.31	1.44	1.77	2.21	2.85	3.54
350	1.28	1.36	1.49	1.85	2.36	3.16	4.44
400	1.32	1.40	1.54	1.92	2.48	3.40	5.17
450	1.36	1.44	1.59	1.98	2.57	3.59	5.75
500	1.40	1.49	1.64	2.04	2.65	3.74	6.21

Table 3: Discrete values of the fitting parameters for Polysilicon.

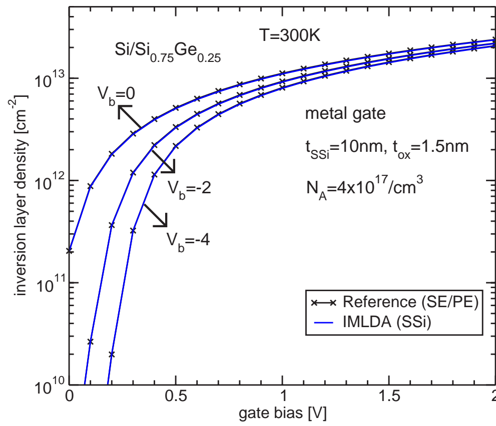

Figure 1: Inversion layer density at room temperature as a function of the gate voltage for three different back bias for metal gate.

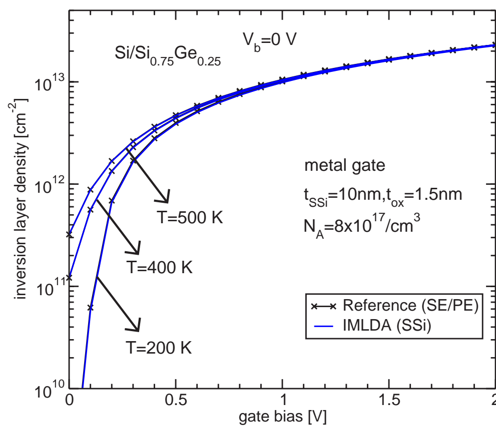

Figure 2: Inversion layer density for three different lattice temperatures and a metal gate.

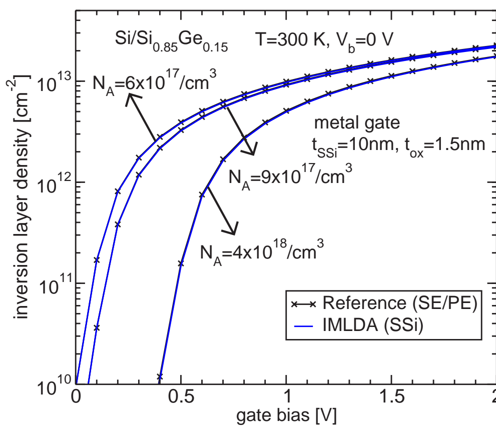

Figure 3: Inversion layer density for three different doping concentrations and a metal gate.

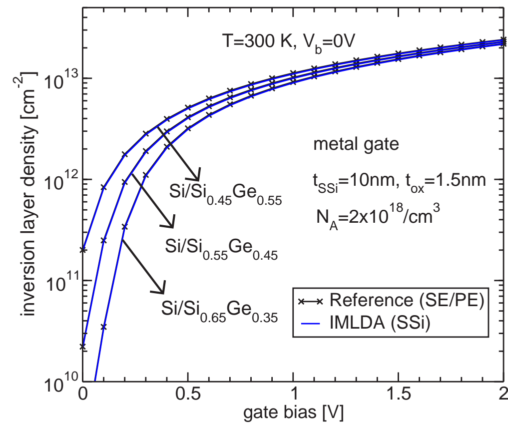

Figure 4: Inversion layer density for three different Ge contents and a metal gate.

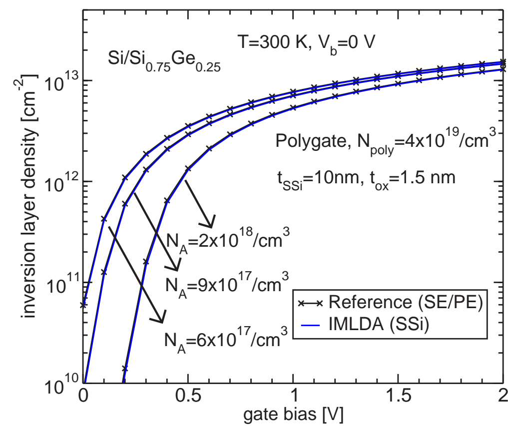

Figure 5: Inversion layer density for three different doping concentrations and a lowly doped polysilicon gate.

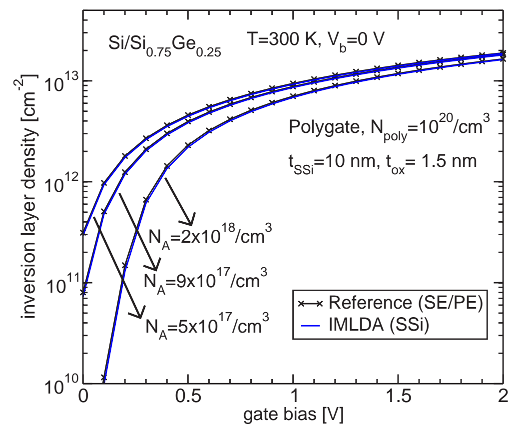

Figure 6: Inversion layer density for three different doping concentrations and a highly doped polysilicon gate with other concentration.